On the other hand, changes in HLA class I expression might by induced by factors other than radiation, e.g., chemotherapy and/or hyperthermia. Gamerio et al. reported that hyperthermia led to a significant increase in major histocompatibility complex (MHC) class I protein expression on the surface of murine colon adenocarcinoma cells that expressed human CEA [22]. In addition, Ohtsukasa et al. reported that anti-cancer drugs (e.g., 5-FU, SN-38, and CDDP) induced a marked increase in MHC class I expression by human colon cancer cell lines cells (COLO 201) *in vitro* [23]. Furthermore, they also reported that anti-cancer drugs induced MHC class I expression in murine colon tumor cells *in vivo*. They thought that this change might be induced by the chemotherapy-induced production of endogenous proteins and/or to increased transport of accumulated material to the cell membrane.

These results suggest that the increased HLA class I expression observed in the present study was augmented by a combination of radiotherapy, chemotherapy, and hyperthermia. Further studies are needed to understand the mechanisms underlying increases in HLA class I expression induced by different treatments; however, this is the first report to show that pre-HCRT increases HLA class I expression in a clinical setting. This result suggests that combination radiotherapy with HLA class I-mediated immunotherapy may amplify weak anti-tumor immune responses caused by loss of HLA class I expression, which is a major mechanism by which tumor cells escape immunosurveillance.

We expected that patients bearing tumors with high HLA class I expression would have a favorable clinical prognosis; however, when we performed univariate analysis, we found no significant positive association between HLA class I expression and OS or DMFS in stage III patients. Moreover, LC showed a significant negative association with post-HCRT HLA class I expression in stage III patients. In contrast to the results presented herein, most previous studies report that patients with tumors showing high HLA class I expression had a better prognosis [3–8]. Additionally, when we investigated the correlation between HCRT-induced changes in HLA class I expression and OS, LC, and DMFS, we found that LC showed a significant negative correlation with increased HLA class I expression. There are several reasons for these discrepancies, as follows: (i) surgical factors may have a stronger impact on clinical prognosis than pre-HCRT-induced HLA class I expression and its immunological effect; (ii) the immunological factors that affect clinical prognosis are quite complex (the effect of HLA class I expression was not strong enough to affect clinical prognosis); and (iii) the number of stage III patients (56) was insufficient to enable a meaningful evaluation of clinical prognosis. Therefore, further studies are required to establish the association between HLA class I expression and prognosis in rectal cancer patients.

In conclusion, the present study suggests that HCRT may increase HLA class I expression by rectal cancer cells; however, multivariate analysis did not show an association between HLA class I expression and prognosis.

Author Contributions

Conceived and designed the experiments: HS YS TN. Performed the experiments: HS MI TO YY NO. Analyzed the data: HS NO TO. Contributed reagents/materials/analysis tools: HS YS SN KA TO YY NO KM TA HK TN. Contributed to the writing of the manuscript: HS YS TN. Obtained permission for use of specimens: TK TA HK.

References

1. Naito Y, Saito K, Shiiba K, Ohuchi A, Saigenji K, et al. (1998) CD8+ T cells infiltrated within cancer cell nests as a prognostic factor in human colorectal cancer. Cancer Res 58: 3491–3494.
2. Khong HT, Restifo NP (2002) Natural selection of tumor variants in the generation of "tumor escape" phenotypes. Nat Immunol 3: 999–1005.
3. Ogino T, Bandoh N, Hayashi T, Miyokawa N, Harabuchi Y, et al. (2003) Association of tapasin and HLA class I antigen down-regulation in primary maxillary sinus squamous cell carcinoma lesions with reduced survival of patients. Clin Cancer Res 9: 4043–4051.
4. Ogino T, Shigyo H, Ishii H, Katayama A, Miyokawa N, et al. (2006) HLA class I antigen down-regulation in primary laryngeal squamous cell carcinoma lesions as a poor prognostic marker. Cancer Res 66: 9281–9289.
5. Kikuchi E, Yamazaki K, Torigoe T, Cho Y, Miyamoto M, et al. (2007) HLA class I antigen expression is associated with a favorable prognosis in early stage non-small cell lung cancer. Cancer Sci 98: 1424–1430.
6. Mizukami Y, Kono K, Maruyama T, Watanabe M, Kawaguchi Y, et al. (2008) Downregulation of HLA Class I molecules in the tumour is associated with a poor prognosis in patients with oesophageal squamous cell carcinoma. Br J Cancer 99: 1462–1467.
7. Homma I, Kitamura H, Torigoe T, Tanaka T, Sato E, et al. (2009) Human leukocyte antigen class I down-regulation in muscle-invasive bladder cancer: its association with clinical characteristics and survival after cystectomy. Cancer Sci 100: 2331–2334.
8. Bandoh N, Ogino T, Katayama A, Takahara M, Katada A, et al. (2010) HLA class I antigen and transporter associated with antigen processing downregulation in metastatic lesions of head and neck squamous cell carcinoma as a marker of poor prognosis. Oncol Rep 23: 933–939.
9. Lee Y, Auh SL, Wang Y, Burnette B, Wang Y, et al. (2009) Therapeutic effects of ablative radiation on local tumor require CD8+ T cells: changing strategies for cancer treatment. Blood 114: 589–595.
10. Takeshima T, Chamoto K, Wakita D, Ohkuri T, Togashi Y, et al. (2010) Local radiation therapy inhibits tumor growth through the generation of tumor-specific CTL: its potentiation by combination with Th1 cell therapy. Cancer Res 70: 2697–2706.
11. Suzuki Y, Mimura K, Yoshimoto Y, Watanabe M, Ohkubo Y, et al. (2012) Immunogenic tumor cell death induced by chemoradiotherapy in patients with esophageal squamous cell carcinoma. Cancer Res 72: 3967–3976.
12. Reits EA, Hodge JW, Herberts CA, Groothuis TA, Chakraborty M, et al. (2006) Radiation modulates the peptide repertoire, enhances MHC class I expression, and induces successful antitumor immunotherapy. J Exp Med 203: 1259–1271.
13. Speetjens FM, de Bruin EC, Morreau H, Zeestraten EC, Putter H, et al. (2008) Clinical impact of HLA class I expression in rectal cancer. Cancer Immunol Immunother 57: 601–609.
14. Garnett CT, Palena C, Chakraborty M, Tsang KY, Schlom J, et al. (2004) Sublethal irradiation of human tumor cells modulates phenotype resulting in enhanced killing by cytotoxic T lymphocytes. Cancer Res 64: 7985–7994.
15. Newcomb EW, Demaria S, Lukyanov Y, Shao Y, Schnee T, et al. (2006) The combination of ionizing radiation and peripheral vaccination produces long-term survival of mice bearing established invasive GL261 gliomas. Clin Cancer Res 12: 4730–4737.
16. Shioya M, Takahashi T, Ishikawa H, Sakurai H, Ebara T, et al. (2011) Expression of hypoxia-inducible factor 1alpha predicts clinical outcome after preoperative hyperthermo-chemoradiotherapy for locally advanced rectal cancer. J Radiat Res 52: 821–827.
17. Tsutsumi S, Tabe Y, Fujii T, Yamaguchi S, Suto T, et al. (2011) Tumor response and negative distal resection margins of rectal cancer after hyperthermochemoradiation therapy. Anticancer Res 31: 3963–3967.
18. Tsukahara T, Kawaguchi S, Torigoe T, Asanuma H, Nakazawa E, et al. (2006) Prognostic significance of HLA class I expression in osteosarcoma defined by anti-pan HLA class I monoclonal antibody, EMR8-5. Cancer Sci 97: 1374–1380.
19. Watson NF, Ramage JM, Madjd Z, Spendlove I, Ellis IO, et al. (2006) Immunosurveillance is active in colorectal cancer as downregulation but not complete loss of MHC class I expression correlates with a poor prognosis. Int J Cancer 118: 6–10.
20. Dunn GP, Bruce AT, Ikeda H, Old LJ, Schreiber RD (2002) Cancer immunoediting: from immunosurveillance to tumor escape. Nat Immunol 3: 991–998.
21. Abdel-Wahab Z, Dar MM, Hester D, Vervaert C, Gangavalli R, et al. (1996) Effect of irradiation on cytokine production, MHC antigen expression, and vaccine potential of interleukin-2 and interferon-gamma gene-modified melanoma cells. Cell Immunol 171: 246–254.
22. Gameiro SR, Higgins JP, Dreher MR, Woods DL, Reddy G, et al. (2013) Combination therapy with local radiofrequency ablation and systemic vaccine enhances antitumor immunity and mediates local and distal tumor regression. PLoS One 8: e70417.
23. Ohtsukasa S, Okabe S, Yamashita H, Iwai T, Sugihara K (2003) Increased expression of CEA and MHC class I in colorectal cancer cell lines exposed to chemotherapy drugs. J Cancer Res Clin Oncol 129: 719–726.

OPEN ACCESS Freely available online

PLOS ONE

Radiotherapy-Induced Anti-Tumor Immunity Contributes to the Therapeutic Efficacy of Irradiation and Can Be Augmented by CTLA-4 Blockade in a Mouse Model

Yuya Yoshimoto[1], Yoshiyuki Suzuki[1]*, Kousaku Mimura[2,4], Ken Ando[1], Takahiro Oike[1], Hiro Sato[1], Noriyuki Okonogi[1], Takanori Maruyama[4], Shinichiro Izawa[4], Shin-ei Noda[1], Hideki Fujii[4], Koji Kono[2,3,4], Takashi Nakano[1]

1 Department of Radiation Oncology, Gunma University Graduate School of Medicine, Maebashi, Japan, **2** Department of Surgery, National University of Singapore, Singapore, Singapore, **3** Cancer Science Institute of Singapore, National University of Singapore, Singapore, Singapore, **4** First Department of Surgery, University of Yamanashi, Yamanashi, Japan

Abstract

Purpose: There is growing evidence that tumor-specific immune responses play an important role in anti-cancer therapy, including radiotherapy. Using mouse tumor models we demonstrate that irradiation-induced anti-tumor immunity is essential for the therapeutic efficacy of irradiation and can be augmented by modulation of cytotoxic T lymphocyte (CTL) activity.

Methods and Materials: C57BL/6 mice, syngeneic EL4 lymphoma cells, and Lewis lung carcinoma (LL/C) cells were used. Cells were injected into the right femurs of mice. Ten days after inoculation, tumors were treated with 30 Gy of local X-ray irradiation and their growth was subsequently measured. The effect of irradiation on tumor growth delay (TGD) was defined as the time (in days) for tumors to grow to 500 mm^3 in the treated group minus that of the untreated group. Cytokine production and serum antibodies were measured by ELISA and flow cytometry.

Results: In the EL4 tumor model, tumors were locally controlled by X-ray irradiation and re-introduced EL4 cells were completely rejected. Mouse EL4-specific systemic immunity was confirmed by splenocyte cytokine production and detection of tumor-specific IgG1 antibodies. In the LL/C tumor model, X-ray irradiation also significantly delayed tumor growth (TGD: 15.4 days) and prolonged median survival time (MST) to 59 days (versus 28 days in the non-irradiated group). CD8(+) cell depletion using an anti-CD8 antibody significantly decreased the therapeutic efficacy of irradiation (TGD, 8.7 days; MST, 49 days). Next, we examined whether T cell modulation affected the efficacy of radiotherapy. An anti-CTLA-4 antibody significantly increased the anti-tumor activity of radiotherapy (TGD was prolonged from 13.1 to 19.5 days), while anti-FR4 and anti-GITR antibodies did not affect efficacy.

Conclusions: Our results indicate that tumor-specific immune responses play an important role in the therapeutic efficacy of irradiation. Immunomodulation, including CTLA-4 blockade, may be a promising treatment in combination with radiotherapy.

Citation: Yoshimoto Y, Suzuki Y, Mimura K, Ando K, Oike T, et al. (2014) Radiotherapy-Induced Anti-Tumor Immunity Contributes to the Therapeutic Efficacy of Irradiation and Can Be Augmented by CTLA-4 Blockade in a Mouse Model. PLoS ONE 9(3): e92572. doi:10.1371/journal.pone.0092572

Editor: Hiroshi Shiku, Mie University Graduate School of Medicine, Japan

Received September 27, 2013; **Accepted** February 24, 2014; **Published** March 31, 2014

Funding: This study was financially supported by MEXT KAKENHI. The funders had no role in study design, data collection and analysis, decision to publish, or preparation of our manuscript.

Competing Interests: The authors have declared that no competing interests exist.

* E-mail: syoshi@med.gunma-u.ac.jp

Introduction

Recently, several reports showed that radiotherapy and anti-tumor immunity are closely associated. We recently demonstrated that tumor antigen-specific T cell responses can be induced in esophageal cancer patients during and after chemoradiotherapy [1]. We detected specific T cells recognizing antigen-derived peptides in a HLA class I-restricted manner using ELISPOT analysis of patient samples [1]. Clinically, the abscopal effect is a well-known but rare phenomenon in which local radiotherapy is associated with the regression of a metastatic tumor located at a distance from the irradiated site. This effect is thought to be mediated by activation of anti-tumor immunity. Postow *et al.* reported a case of the abscopal effect in a patient with melanoma treated with radiotherapy and ipilimumab, an antagonistic antibody against cytotoxic T-lymphocyte-associated antigen 4 (CTLA-4). In this case, disease resolution after radiotherapy was associated with a specific antibody response [2]. Demaria *et al.* used a mouse syngeneic mammary carcinoma model to show that abscopal effects result from irradiation-activated anti-tumor immunity [3]. Taken together, these observations indicate that

local radiotherapy can induce systemic tumor-specific immune responses.

The molecular mechanisms that mediate anti-tumor immunity, in terms of irradiation-induced immunogenic tumor cell death and its impact on the prognosis of cancer patients, have also been investigated. Apetoh *et al.* reported that activation of tumor antigen-specific T cell responses involve the secretion of high-mobility-group box 1 (HMGB1) alarmin protein from dying tumor cells and the action of HMGB1 on Toll-like receptor 4 (TLR4)-expressing dendritic cells [4]. This pathway and activated anti-tumor immunity play important roles in human cancer, as patients with breast cancer who carry a *TLR4* loss-of-function allele relapse more quickly after radiotherapy and chemotherapy. HMGB1 may also be a prognostic factor; its up-regulation within the tumor microenvironment is positively correlated with esophageal cancer patient survival after chemoradiotherapy [1], although the significance of HMGB1 is still controversial. Thus, radiotherapy-induced immune responses may contribute to the therapeutic efficacy of irradiation. However, the immune system does not always exert robust responses, such as the abscopal effect, suggesting the existence of suppressor mechanisms. Regulatory T (Treg) cells mediate one of the most important mechanisms for suppression of effector T cell responses. Treg cells are characterized as CD4(+)CD25(+)FoxP3(+) and have a critical role in the maintenance of immunological self-tolerance [5]. Treg cells suppress effector cells by co-localizing Treg and effector cells with antigen presenting cells [6], and also by inhibiting the release of cytolytic granules from effector T cells [7]. Cancer patients have increased levels of Treg cells, resulting in poor immune responses to tumors. Thus, Treg cell depletion may be an effective cancer treatment [5].

In this study, we used mouse models and immunomodulatory antibodies to test whether irradiation-induced anti-tumor responses are essential for the efficacy of irradiation and whether this effect can be augmented by T cell modulation.

Materials and Methods

Mice, cell lines and antibodies

C57BL/6 mice and BALB/c-*nu/nu* mice were purchased from Japan SLC (Shizuoka, Japan). Mice were bred and maintained under specific-pathogen-free conditions. C57BL/6 syngeneic Lewis lung carcinoma cells (LL/C; mouse lung squamous carcinoma) were purchased from American Type Culture Collection (Manassas, VA). Cells were cultured in RPMI 1640 supplemented with 5% fetal calf serum (FCS), 50 U/ml penicillin, and 2 mM L-glutamine. RPMI 1640 and FCS were purchased from Invitrogen (Carlsbad, CA) and penicillin was purchased from Sigma-Aldrich (St. Louis, MO). All procedures for the care and treatment of animals were performed according to the Japanese Act on the Welfare and Management of Animals and the Guidelines for the Proper Conduct of Animal Experiments issued by the Science Council of Japan. The experimental protocol was approved by the Institutional Committee of Gunma University (09-074). Every effort was made to minimize animal suffering and the number of animals used. Anti-mouse CD8 (clone 53.6.72), anti-mouse folate receptor 4 (FR4; clone TH6), anti-mouse glucocorticoid-induced tumor necrosis factor receptor family-related gene (GITR; clone DTA-1), and anti-mouse CTLA-4 (clone 9H10) antibodies were purchased from eBioscience (San Diego, CA).

Local irradiation, measurement of tumor volume, and immunomodulatory antibody treatment

C57BL/6 mice and the syngeneic cell lines, LL/C, EL4, and B16 were used. Cells (5×10^5) were injected into the right/bilateral hind limbs of C57BL/6 mice. When tumors reached 100 mm^3 in volume, they were exposed to 30 Gy of X-rays at a dose rate of 1.3 Gy/min (TITAN-225S, Shimazu, Japan). Only tumors were irradiated; the rest of the body was shielded by lead. Tumor size was measured using calipers every other day. Tumor volume (V) was calculated using the following formula: $V = ab^2/2$ (where a is the long axis diameter and b is the short axis diameter). The effect of irradiation on tumor growth time, the 'tumor growth delay' (TGD), was defined as the time in days for tumors to grow to 500 mm^3 in the treated group minus that in the untreated group. To examine the effect of immunomodulatory antibodies, anti-mouse CD8 antibody (administered intravenously at a dose of 66 μg/mouse on Days 1, 6, and 10), anti-CTLA-4 antibody (administered intraperitoneally at a dose of 200 μg/mouse on Days 1, 4, and 7), anti-FR4 antibody (administered intravenously at a dose of 10 μg/mouse on Days 1, 4, and 7), anti-GITR antibody (administered intratumorally at a dose of 50 μg/mouse on Day 1), and saline (for the non-treated group, administered intravenously on Days 1, 4, and 7) were used.

ELISA

To evaluate splenocyte function, EL4 tumors borne by C57BL/6 and BALB/c-*nu/nu* mice were exposed to 30 Gy of X-rays. Irradiated non-tumor-bearing C57BL/6 and BALB/c-nu/nu mice were used as controls. Spleens were removed at 0, 10, 11, 14, 17, 20 and 24 days after the first tumor cell inoculation and splenocytes (3.0×10^6/ml) were co-cultured with irradiated EL4 cells (0.3×10^6/ml) in medium for 24 h. IFN-γ and TNF-α levels in the culture supernatant were then measured using mouse IFN-γ (R&D Systems, Minneapolis) and TNF-α (R&D Systems) ELISA kits, according to the manufacturers' instructions. To measure HMGB1 concentrations, LL/C and EL4 cells were seeded in culture dishes, exposed to X-rays (Siemens-Asahi Medical Technologies, Tokyo, Japan), and then cultured in RPMI for 48 h. Culture supernatants were collected and HMGB1 concentrations were measured using an ELISA kit (Shinotest, Tokyo, Japan) according to the manufacturer's instructions.

Flow cytometric analysis of EL4-specific antibodies

Blood samples were taken from mice described in the previous section 24 days after tumor inoculation. Serum was obtained from blood samples by centrifugation. The serum was diluted 1:5 with phosphate-buffered saline (PBS) and incubated with EL4 cells for 30 min on ice. EL4 cells were then washed and stained with FITC-conjugated anti-mouse IgG1 (eBioscience). Stained cells were analyzed by four-color flow cytometry using a FACSCalibur flow cytometer (BD Biosciences). Data were analyzed using CellQuest™ software (BD Biosciences).

Statistical analysis

Statistical analysis was performed using two-tailed, unpaired Student's *t* tests. Error bars represent the standard deviation (SD). For survival curves, statistical analyses were performed using the log-rank (Mantel-cox) test. All statistical analyses were performed using IBM SPSS Statistics software, version 21. A p value <0.05 was considered significant.

Results

Irradiation of EL4 tumors prevented systemic tumor progression and led to the rejection of re-inoculated tumors in C57BL/6 mice, but not in BALB/c-nu/nu mice

First, the therapeutic effect of X-ray irradiation against EL4 tumors was tested. EL4 tumors were locally controlled by 30 Gy of X-ray irradiation. Irradiation induced a significant decrease in tumor volume ($p<0.01$) and almost all irradiated mice survived (one-fifth died due to marginal recurrence), while non-irradiated mice died within 5–8 weeks of inoculation (Fig. 1A, 1B). Dissections revealed that all mice had significant lymph node metastasis. Liver and lung metastasis was macroscopically less obvious (Fig. 1C). Irradiated mice completely rejected re-inoculated EL4 cells administered 24 days after the first inoculation. EL4 cells were not rejected when B16 melanomas were used in the first inoculation (Fig. 1D). Although irradiation resulted in a reduction in EL4 tumor size in BALB/c-*nu/nu* mice, all animals died within 3 weeks of irradiation (Fig. 2A, 2B). In these cases, systemic tumor metastasis (lymph nodes, lung and liver) was observed (Fig. 2C).

EL4-specific cellular and humoral immunity was induced in irradiated EL4-bearing C57/BL6 mice

To examine cellular immunity in treated mice, splenocyte cytokine production was measured. Splenocytes of irradiated EL4-bearing C57/BL6 mice, but not those of irradiated non-tumor-bearing C57/BL6 mice, produced significant amounts of IFN-γ and TNF-α (Fig. 3A). There was no significant production of these cytokines by splenocytes from either tumor-bearing or non-tumor-bearing nude mice (Fig. 3A). In a time-course study, cytokine production was higher in tumor-bearing mice (Day 10, before irradiation) than in non-tumor-bearing mice (Day 0). After irradiation, cytokine production decreased on Days 11 and 14. However, cytokine production then increased on Days 17 and 20 (Figure 3B). Humoral immunity was examined by flow cytometry. EL4-specific IgG1 was detected in the serum of irradiated EL4-bearing C57/BL6 mice (Fig. 3C). Thus, both cellular and humoral immunity against EL4 tumors were induced in irradiated EL4-bearing C57/BL6 mice. Anti-tumor effects of the immune response against EL4 tumors were also examined *in vivo*. EL4 tumors were inoculated into both the right and left hind limbs; however, only the tumors in the right hind limbs were irradiated. All of the irradiated tumors disappeared within 7 days of irradiation. In addition, irradiation inhibited the growth of the non-irradiated tumors in the left hind limbs; the volumes were significantly smaller than those in control mice on Day 19 post-inoculation ($p<0.01$) (Figure 4). There was no significant difference in tumor growth between the unilaterally inoculated tumors and either of the bilaterally inoculated tumors in non-irradiated mice (Supplemental Figure S1).

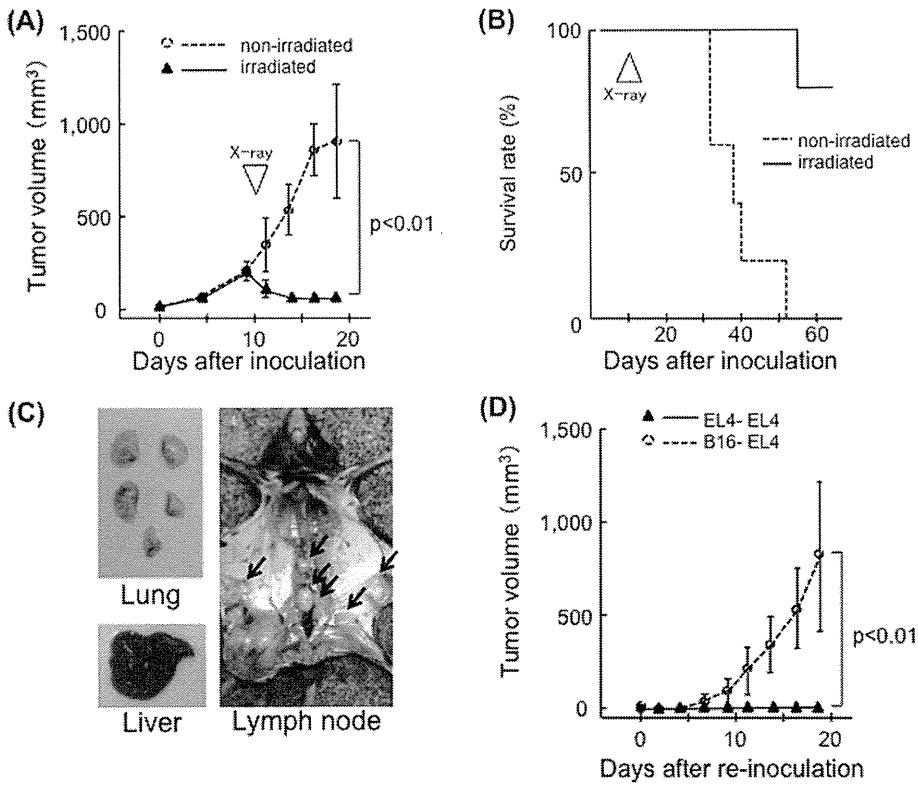

Figure 1. Therapeutic effects of X-ray irradiation on EL4 tumors in C57BL/6 mice. (A) Growth curves of EL4 tumors in the non-treated group (open circles, n = 5) and irradiated group (closed triangles, n = 5). X-ray irradiation was performed on Day 10; bars, SD. (B) Survival curves for EL4-inoculated C57BL/6 mice, the non-treated group (dotted line), and the irradiated group (solid line). (C) Lymph node metastasis (arrows) in a representative mouse 20 days after tumor inoculation. (D) Growth curve of EL4 tumors (second inoculation). EL4 cells were re-inoculated into the left hind limbs of mice 24 days after the first challenge with EL4 cells (closed triangles, n = 5) or B16 cells (open circles, n = 5); bars, S.D.
doi:10.1371/journal.pone.0092572.g001

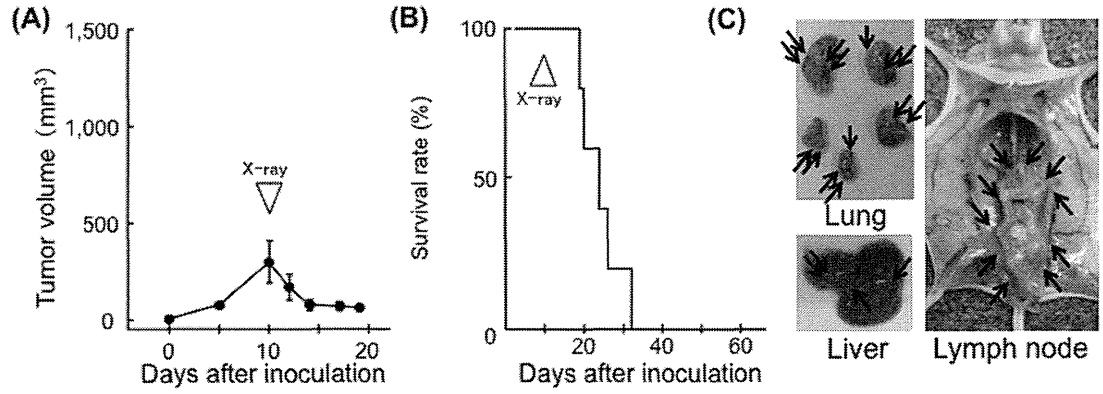

Figure 2. Effect of X-ray irradiation on EL4 tumors in BALB/c-nu/nu mice. (A) Growth curves of EL4 tumors in the irradiated group (n = 5). X-ray irradiation was performed on Day 10; bars, SD. (B) Survival curves for EL4-inoculated BALB/c-*nu/nu* mice. (C) Systemic metastases (arrows) in the internal organs of a representative mouse 20 days after tumor inoculation.
doi:10.1371/journal.pone.0092572.g002

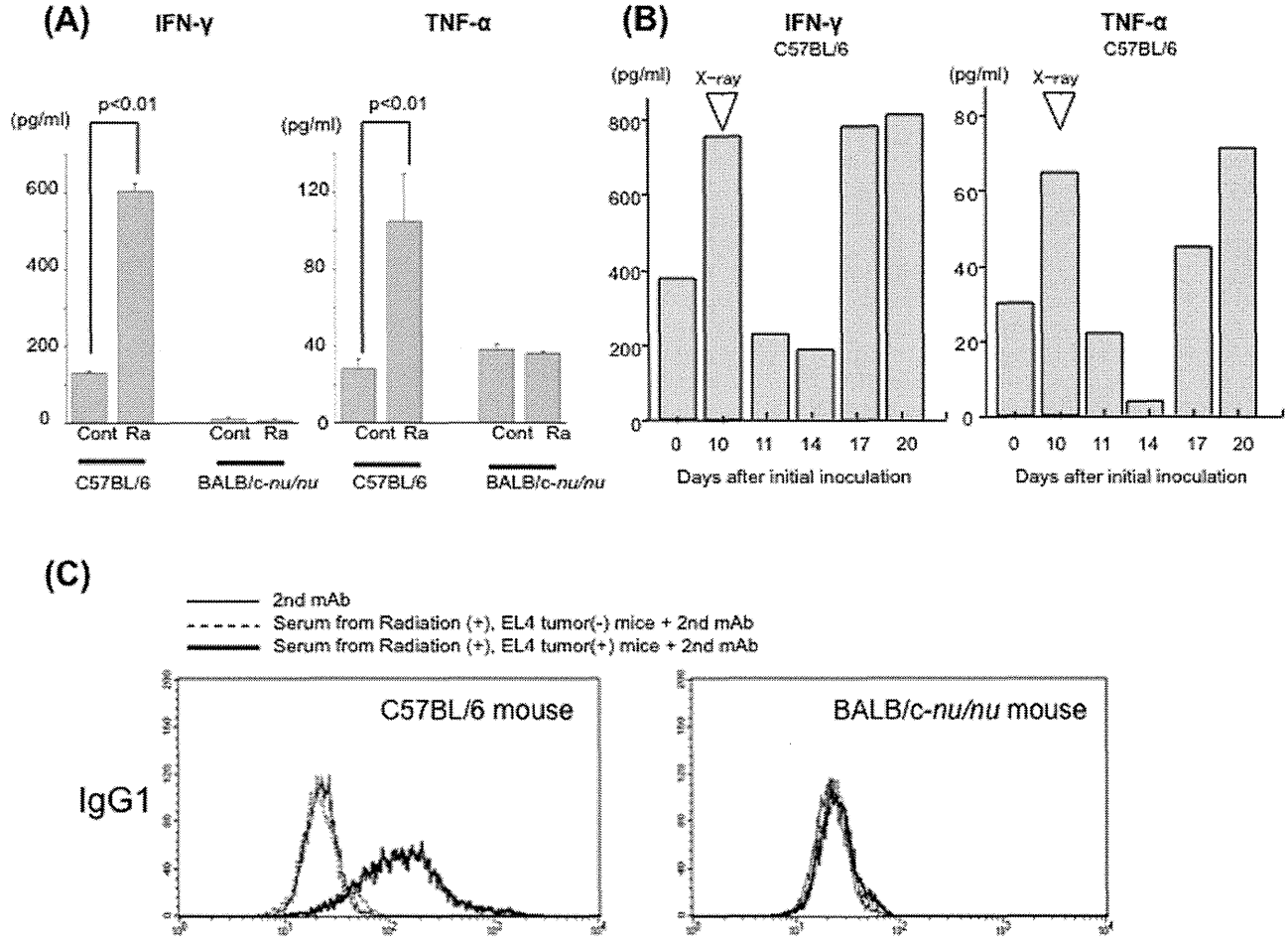

Figure 3. Immune reaction in irradiated EL4 tumor-bearing mice. (A) IFN-γ (left) and TNF-α (right) concentrations in C57BL/6 and BALB-c *nu/nu* mouse splenocyte culture supernatants as measured by ELISA. Mice were sacrificed 24 days after tumor inoculation. Control (cont) splenocytes from non-tumor-bearing irradiated mice; Ra, splenocytes from irradiated EL4 tumor-bearing mice. (B) Mice were sacrificed on the indicated day and splenocytes were cultured for ELISA. Irradiation was performed on Day 10. Day 0, splenocytes from non-tumor-bearing non-irradiated mice; Day 10, tumor-bearing non-irradiated mice; Days 11, 14, 17, 20, tumor-bearing irradiated mice. (C) Antibodies specific for EL4 cells produced by local irradiation of EL4 tumors in C57/BL6 (left) and BALB/c-nu/nu (right) mice.
doi:10.1371/journal.pone.0092572.g003

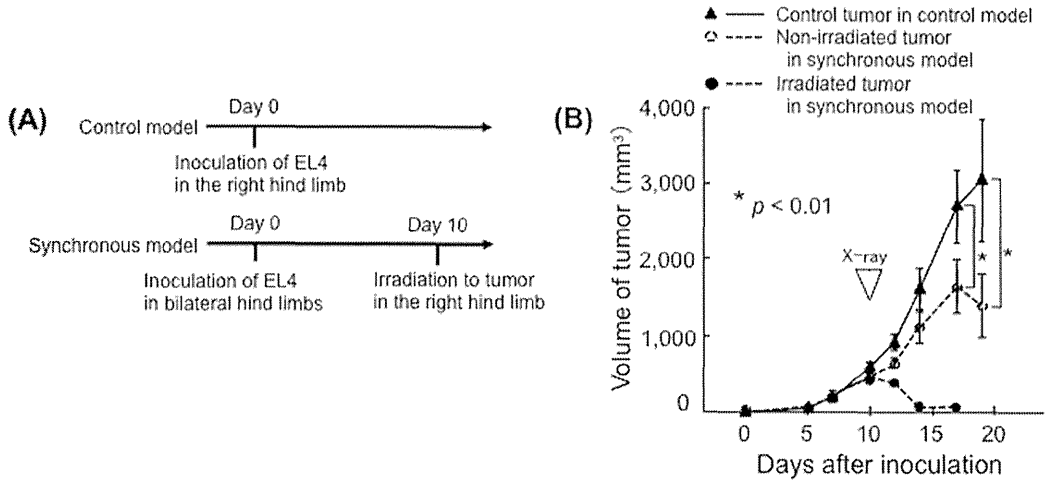

Figure 4. Irradiation of EL4 tumors in C57BL/6 mice results in the abscopal effect. (A) Timing of primary EL4 cell inoculation and tumor irradiation in control and synchronous models. (B) Volume of irradiated tumors in the right hind limbs of synchronous model mice (closed circles, n = 5) and of non-irradiated tumors in the left hind limbs of synchronous model mice (open circles) and the control tumors in control model mice (closed triangles, n = 5); bars, S.D.
doi:10.1371/journal.pone.0092572.g004

Irradiation delayed LL/C tumor growth in C57BL/6 mice and the therapeutic efficacy of irradiation was reduced by depleting CD8-positive lymphocytes

Next, we evaluated tumor growth and survival times using an LL/C tumor model. Tumors were treated with 30 Gy of X-ray irradiation when they reached a volume of 100 mm^3. Growth was significantly delayed by irradiation, with volumes reaching 500 mm^3 at 28.7±2.2 days post-irradiation compared with 13.2±1.7 days in the non-irradiated group; hence the TGD was 15.4 days (Fig. 5A). To examine the involvement of immunity, we used a neutralizing anti-CD8 antibody. Depletion of CD8(+) cells using this antibody significantly decreased the TGD to 8.7±3.2 days ($p<0.001$; Fig. 5A). Median survival time (MST) in the anti-CD8 antibody plus irradiation group was 49 days (95% confidence interval [CI], 41.3–56.7), while that of the irradiation alone group was 59 days (95% CI, 51.3–66.7). Thus, CD8(+) cell depletion also significantly reduced survival time ($p<0.01$; Fig. 5B). Tumor growth and survival time were not markedly different between the anti-CD8 antibody alone group and the control group.

CTLA-4 blockade enhanced the efficacy of irradiation in a mouse tumor model

We next examined whether an immunomodulatory antibody affected the efficacy of radiotherapy (Fig. 6A, 6B). Among the antibodies tested, an anti-CTLA-4 antibody significantly increased the anti-tumor efficacy of irradiation, with the TGD extended from 13.1±2.3 (irradiation alone group) to 19.5±2.9 (anti-CTLA-4 antibody plus irradiation group) days ($p<0.005$; Fig. 6A). Survival time was also longer in the anti-CTLA-4 antibody plus irradiation group (MST, 56 days; 95% CI, 51.7–60.3) than in the irradiation alone group (MST, 46 days; 95% CI, 43.4–48.6; $p<0.05$; Fig. 6B). Tumor growth and survival time were not markedly different between the anti-CTLA-4 antibody alone group and the control group (Fig. 6). The TGD and survival times of irradiated groups treated with anti-FR4 or anti-GITR antibodies did not differ significantly from those of the control group (Fig. 6). The average tumor volume tended to be slightly lower in the anti-GITR plus irradiation group than in the irradiation alone group; however, this was not statistically significant.

X-ray irradiation induced secretion of HMGB1 protein from LL/C and EL4 cells *in vitro*

It was recently reported that X-ray irradiation-induced immunogenic cell death involves the secretion of HMGB1. Therefore, we examined whether X-ray irradiation induces HMGB1 release from LL/C and EL4 cells. Notably, HMGB1 was detected in the culture medium of irradiated LL/C cells 48 h after irradiation. Dose-dependent effects were observed: 2 Gy irradiation had no significant effect on HMGB1 release from LL/C cells, whereas higher doses (6 Gy and 30 Gy) induced greater amounts of HMGB1 (Figure 7). Similar results were obtained when EL4 cells were used (Figure 7). Thus, X-ray irradiation induces immunogenic cell death in these cells.

Discussion

In the present study, we demonstrated that EL4 tumor-bearing mice acquired EL4-specific immunity after irradiation. Localized irradiation of tumors did not extend survival and did not induce EL4-specific immunity in nude mice. The role of the immune system was further confirmed using a LL/C tumor model. The efficacy of radiotherapy for treating LL/C tumors was reduced by depleting CD8(+) cells, with both TGD and survival time being significantly reduced. These results clearly indicate that CD8(+) cell activity influences the efficacy of radiotherapy. In addition, the efficacy of irradiation was augmented by anti-CTLA-4 antibody treatment.

Recent evidence suggests that anti-tumor immunity can be induced by radiotherapy. Furthermore, tumor-specific immune responses induced by irradiation play a crucial role in successful radiotherapy. Lee *et al.* recently reported that irradiation increases T cell priming, leading to tumor reduction in syngeneic models of B16 melanoma [8]. Takeshima *et al.* reported that CD8(+) cell depletion decreases the therapeutic efficacy of irradiation in a C57BL/6 mouse tumor model that used ovalbumin-transfected cells [9]. In the present study, C57BL/6 mice were inoculated with EL4 cells and then irradiated. Irradiation-induced anti-tumor

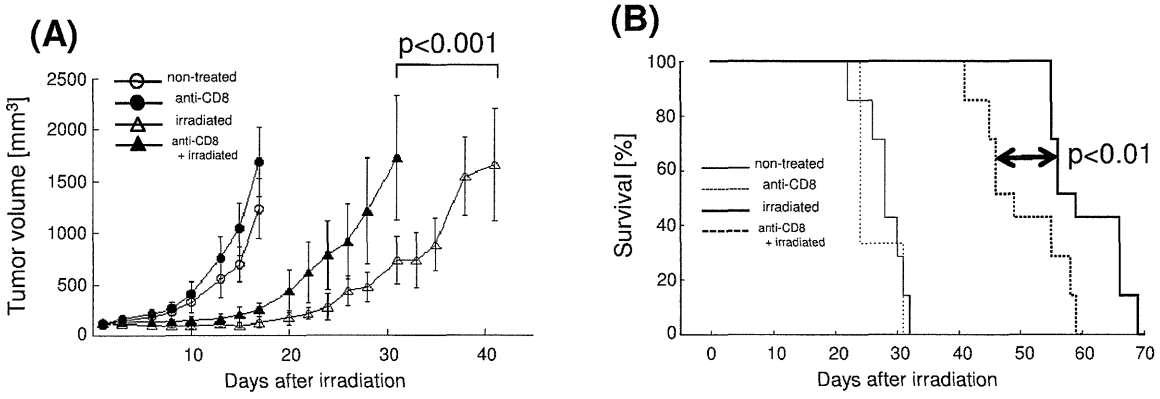

Figure 5. X-ray irradiation delays LL/C tumor growth, and CTL depletion reduces TGD, in C57BL/6 mice. (A) Growth curves of LL/C tumors in the non-treated group (open circles, n = 7), irradiated group (open triangles, n = 7), anti-CD8 antibody-treated group (closed circles, n = 3), and irradiation plus anti-CD8 antibody-treated group (closed triangles, n = 7). X-ray irradiation was performed when tumors reached 100 mm^3 in volume (Day 0); bars, SD. (B) Survival curves for LL/C-inoculated C57BL/6 mice, non-treated group (thin solid line), irradiated group (thick solid line), anti-CD8 antibody-treated group (thin dotted line), and irradiation plus anti-CD8 antibody-treated group (thick dotted line).
doi:10.1371/journal.pone.0092572.g005

immunity was confirmed by the following observations: (i) re-inoculated EL4 cells were completely rejected, (ii) EL4-specific cellular and humoral immunity was detected, and (iii) when mice were inoculated with tumors in both hind limbs, irradiation of one tumor caused shrinkage of the other, indicating an abscopal effect. We further quantified immune responses in an LL/C tumor model. Depleting CD8(+) cells using an anti-CD8 antibody significantly reduced the therapeutic efficacy of irradiation in terms of both tumor growth and survival time. These results demonstrate that local irradiation induces systemic tumor-specific immune responses, which are also essential for the local control of tumors. We emphasize that irradiation delayed tumor growth as a result of tumor-specific immune responses, not solely because of DNA breakage.

The results of this study, which demonstrate that activation of CD8(+) immune cells is involved in the efficacy of irradiation, suggest that therapeutic efficacy could be increased by augmenting the immune response. There are several approaches to activating anti-tumor immunity. The most promising procedure is immunomodulation using specific antibodies. Thus, we examined the effect of immunomodulatory antibodies on the efficacy of irradiation. Among the antibodies tested, an anti-CTLA-4 antibody increased the efficacy of irradiation, leading to increases in both TGD and survival time. CTLA-4 is expressed exclusively on T cells, where it primarily regulates the amplitude of the early stages of T cell

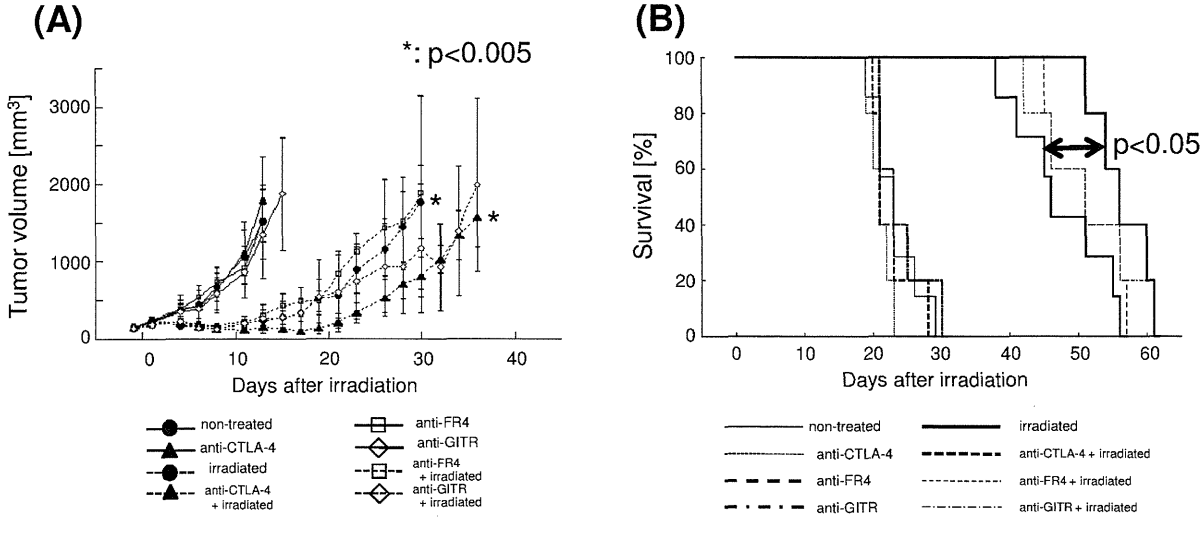

Figure 6. X-ray irradiation delays LL/C tumor growth and antibody-mediated immunomodulation increases TGD in C57BL/6 mice. (A) Growth curves of LL/C tumors in non-irradiated (solid line, n = 5/each group) and irradiated (dashed line, n = 5/each group) groups. Effects of the anti-CTLA-4 (closed triangles), anti-FR4 (open squares), anti-GITR (open diamonds) immunomodulatory antibodies, and the saline control (for the non-treated group, closed circles) were examined. X-ray irradiation was performed when tumors reached 100 mm^3 in volume (Day 0); bars, SD. (B) Survival curves for each group of LL/C-inoculated C57BL/6 mice; non-treated (thin solid line), irradiated (thick solid line), anti-CTLA-4 antibody-treated (thin dotted line), irradiation plus anti-CTLA-4 antibody-treated (thick dotted line), anti-FR4 antibody-treated (thick dashed line), irradiation plus anti-FR4 antibody-treated (thin dashed line), anti-GITR antibody-treated (thick dash-dotted line), and irradiation plus anti-GITR antibody-treated (thin dash-dotted line).
doi:10.1371/journal.pone.0092572.g006

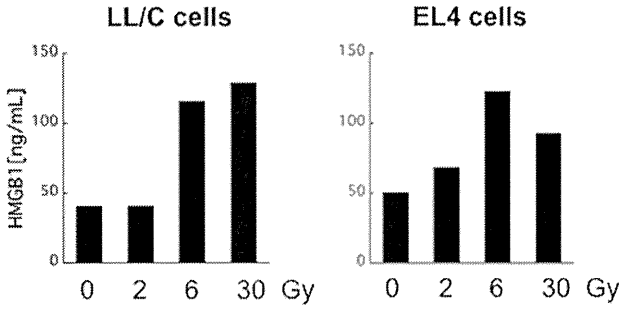

Figure 7. X-ray irradiation induces HMGB1 protein *in vitro.* Cells were exposed to the indicated doses of X-ray irradiation and then cultured for 48 h. HMGB1 concentrations in culture supernatants were measured by ELISA.
doi:10.1371/journal.pone.0092572.g007

activation. CTLA-4 blockade broadly enhances immune responses in animal models, including systemic immune hyperactivation and anti-tumor immunity. This increase in anti-tumor activity by CTLA-4 blockade is due to a combination of direct activation of effector T cell function and concomitant inhibition of regulatory T cell (Treg) activity [10–12]. Dewan *et al.* reported that the combined use of local irradiation and CTLA-4 blockade inhibits metastases in a mouse model of breast cancer [13]. The same group also reported that an anti-CTLA-4 antibody can induce an experimental abscopal effect in mouse models [14]. Taken together with our results, these findings indicate that irradiation-induced anti-tumor immunity can be augmented by CTLA-4 blockade and that the resulting enhanced immunity acts both locally and systemically. In initial studies, significant anti-tumor responses were observed in mice bearing immunogenic tumors; however, poorly immunogenic tumors did not respond to anti-CTLA-4 antibody monotherapy [10]. This is in agreement with our results demonstrating that the anti-tumor effect of the anti-CTLA-4 antibody was only observed when it was combined with irradiation. Thus, a combination of irradiation and anti-CTLA-4 antibody treatment may be an attractive approach. Clinically, a combination of local irradiation and anti-CTLA-4 antibody therapy caused regression of metastatic tumors at a distance from the irradiated site (abscopal effect) in a melanoma patient [2]. This tumor regression was associated with antibody responses against a tumor-specific cancer testis antigen, suggesting that augmentation of tumor-specific immune responses had occurred and demonstrating the promise of a combination of radiotherapy and CTLA-4 blockade in a clinical setting.

Several studies document tumor rejection following the depletion of Treg cells. Treg cells express high levels of FR4 and an anti-FR4 antibody specifically reduces Treg cell levels, thereby inducing effective anti-tumor immunity in tumor-bearing mice [15]. Treg cells also express high levels of GITR, and an agonistic antibody, DTA1, is an effective anti-tumor agent. When injected intratumorally, DTA1 exerts its anti-tumor activity by inhibiting the suppressor function of Treg cells [16,17]. However, these two antibodies had no significant effect on the efficacy of irradiation in our investigation. One possible explanation is that the anti-CTLA-4 antibody inhibits Treg activity while also increasing the activity of effector cells such as CTLs, whereas the anti-FR4 antibody and DTA1 may not. Thus, in our *in vivo* model, it is possible that the anti-CTLA-4 antibody augmented both Treg depletion and effector cell activity. Another report noted that experimental outcomes can be influenced by the timing and dose of antibody administration [18]. Further studies are required to optimize the dose and timing of antibody administration when used in combination with irradiation.

In conclusion, this study demonstrates that tumor-specific immune responses play an important role in the therapeutic efficacy of irradiation, which can be augmented by immune checkpoint (CTLA-4) inhibition. The combination of radiotherapy and CTLA-4 blockade is a promising potential cancer therapy, although further study is required.

Supporting Information

Figure S1 Growth of EL4 tumor in unilateral and bilateral models. (A) Timing of primary EL4 cell inoculation in unilateral and bilateral models. (B) Volume of tumors in right hind limbs of unilateral model mice (closed circles, n = 7), and tumors in right hind limbs of the bilateral model mice (open circles) and tumors of in left hind limb of the bilateral model mice (closed triangles, n = 7); bars, S.D.
(TIFF)

Acknowledgments

EL4 cells and B16 cells were kind gifts from Prof. Rolf Kiessling (Department of Oncology and Pathology, Immune and Gene Therapy Laboratory, Cancer Center Karolinska, Karolinska Institutet, Stockholm, Sweden).

Author Contributions

Conceived and designed the experiments: YY YS KM HF KK TN. Performed the experiments: YY YS KM KA TO HS NO TM SI SN. Analyzed the data: YY YS KM KA TO HS NO TM SI SN. Contributed reagents/materials/analysis tools: YY YS KM KA TO HS NO TM SI SN. Wrote the paper: YY YS KM HF KK TN.

References

1. Suzuki Y, Mimura K, Yoshimoto Y, Watanabe M, Ohkubo Y, et al. (2012) Immunogenic tumor cell death induced by chemoradiotherapy in patients with esophageal squamous cell carcinoma. Cancer Res 72: 3967–3976.
2. Postow MA, Callahan MK, Barker CA, Yamada Y, Yuan J, et al. (2012) Immunologic correlates of the abscopal effect in a patient with melanoma. N Engl J Med 366: 925–931.
3. Demaria S, Ng B, Devitt ML, Babb JS, Kawashima N, et al. (2004) Ionizing radiation inhibition of distant untreated tumors (abscopal effect) is immune mediated. Int J Radiat Oncol Biol Phys 58: 862–870.
4. Apetoh L, Ghiringhelli F, Tesniere A, Obeid M, Ortiz C, et al. (2007) Toll-like receptor 4-dependent contribution of the immune system to anticancer chemotherapy and radiotherapy. Nat Med 13: 1050–1059.
5. von Boehmer H and Daniel C (2013) Therapeutic opportunities for manipulating Treg cells in autoimmunity and cancer. Nat Rev Drug Discovery, 12, 51–63.
6. Verginis P, McLaughlin KA, Wucherpfennig KW, von Boehmer H and Apostolou I (2008) Induction of antigen-specific regulatory T cells in wild-type mice: visualization and targets of suppression. Proc Natl Acad Sci USA, 105, 3479–3484.
7. Mempel TR, Pittet MJ, Khazaie K, Weninger W, Weissleder R, et,al. (2006) Regulatory T cells reversibly suppress cytotoxic T cell function independent of effector differentiation. Immunity, 25, 129–141.
8. Lee Y, Auh SL, Wang Y, Burnette B, Wang Y, et al. (2009) Therapeutic effects of ablative radiation on local tumor require CD8+ T cells: changing strategies for cancer treatment. Blood 114: 589–595.
9. Takeshima T, Chamoto K, Wakita D, Ohkuri T, Togashi Y, et al. (2010) Local radiation therapy inhibits tumor growth through the generation of tumor-specific CTL: its potentiation by combination with Th1 cell therapy. Cancer Res 70: 2697–2706.
10. Pardoll DM. (2012) The blockade of immune checkpoints in cancer immunotherapy. Nat Rev Cancer 12: 252–264.

11. Peggs KS, Quezada SA, Chambers CA, Korman AJ, Allison JP (2009) Blockade of CTLA-4 on both effector and regulatory T cell compartments contributes to the antitumor activity of anti-CTLA-4 antibodies. J Exp Med 206: 1717–1725.
12. Grosso JF, Jure-Kunkel MN. (2013) CTLA-4 blockade in tumor models: an overview of preclinical and translational research. Cancer immunity 13: 5–18.
13. Demaria S, Kawashima N, Yang AM, Devitt ML, Babb JS, et al. (2005) Immune-mediated inhibition of metastases after treatment with local radiation and CTLA-4 blockade in a mouse model of breast cancer. Clin Cancer Res 11: 728–734.
14. Dewan MZ, Galloway AE, Kawashima N, Dewyngaert JK, Babb JS, et al. (2009) Fractionated but not single-dose radiotherapy induces an immune-mediated abscopal effect when combined with anti-CTLA-4 antibody. Clin Cancer Res 15: 5379–5388.
15. Yamaguchi T, Hirota K, Nagahama K, Ohkawa K, Takahashi T, et al. (2007) Control of immune responses by antigen-specific regulatory T cells expressing the folate receptor. Immunity 27: 145–159.
16. Ko K, Yamazaki S, Nakamura K, Nishioka T, Hirota K, et al. (2005) Treatment of advanced tumors with agonistic anti-GITR mAb and its effects on tumor-infiltrating Foxp3+CD25+CD4+ regulatory T cells. J Exp Med 202: 885–891.
17. Schaer DA, Murphy JT, Wolchok JD (2012) Modulation of GITR for cancer immunotherapy. Curr Opin Immunol 24: 217–224.
18. Takeda K, Kojima Y, Uno T, Hayakawa Y, Teng MWL, et al. (2010) Combination therapy of established tumors by antibodies targeting immune activating and suppressing molecules. J Immunol 184: 5493–5501.

PLOS | ONE

RESEARCH ARTICLE

Carbon-Ion Beam Irradiation Kills X-Ray-Resistant p53-Null Cancer Cells by Inducing Mitotic Catastrophe

Napapat Amornwichet[1,2], Takahiro Oike[1,3]*, Atsushi Shibata[4], Hideaki Ogiwara[3], Naoto Tsuchiya[3], Motohiro Yamauchi[5], Yuka Saitoh[1], Ryota Sekine[4], Mayu Isono[6], Yukari Yoshida[6], Tatsuya Ohno[6], Takashi Kohno[3], Takashi Nakano[1]

1. Department of Radiation Oncology, Gunma University Graduate School of Medicine, Maebashi, Gunma, Japan, **2.** Department of Radiology, Chulalongkorn University, Pathumwan, Bangkok, Thailand, **3.** Division of Genome Biology, National Cancer Center Research Institute, Chuo-ku, Tokyo, Japan, **4.** Advanced Scientific Research Leaders Development Unit, Gunma University, Maebashi, Gunma, Japan, **5.** Division of Radiation Biology and Protection, Atomic Bomb Disease Institute, Nagasaki University, Sakamoto, Nagasaki, Japan, **6.** Gunma University Heavy Ion Medical Center, Maebashi, Gunma, Japan

*oiketakahiro@gmail.com

OPEN ACCESS

Citation: Amornwichet N, Oike T, Shibata A, Ogiwara H, Tsuchiya N, et al. (2014) Carbon-Ion Beam Irradiation Kills X-Ray-Resistant p53-Null Cancer Cells by Inducing Mitotic Catastrophe. PLoS ONE 9(12): e115121. doi:10.1371/journal.pone.0115121

Editor: Peiwen Fei, University of Hawaii Cancer Center, United States of America

Received: July 17, 2014

Accepted: November 18, 2014

Published: December 22, 2014

Data Availability: The authors confirm that all data underlying the findings are fully available without restriction. All relevant data are within the paper and its Supporting Information files.

Funding: This work was supported by Grants-in-Aid from the Ministry of Education, Culture, Sports, Science, and Technology of Japan for programs for Leading Graduate Schools, Cultivating Global Leaders in Heavy Ion Therapeutics and Engineering, and for Strategic Young Researcher Overseas Visits Program for Accelerating Brain Circulation, and Scientific Research on Innovative Areas (22131006). This work was also supported by Grants-in-Aid from the Japan Society for the Promotion of Science for Young Scientists (B) KAKENHI [10643471]. The funders had no role in study design, data collection and analysis, decision to publish, or preparation of the manuscript.

Competing Interests: The authors have declared that no competing interests exist.

Abstract

Background and Purpose: To understand the mechanisms involved in the strong killing effect of carbon-ion beam irradiation on cancer cells with *TP53* tumor suppressor gene deficiencies.

Materials and Methods: DNA damage responses after carbon-ion beam or X-ray irradiation in isogenic HCT116 colorectal cancer cell lines with and without *TP53* ($p53^{+/+}$ and $p53^{-/-}$, respectively) were analyzed as follows: cell survival by clonogenic assay, cell death modes by morphologic observation of DAPI-stained nuclei, DNA double-strand breaks (DSBs) by immunostaining of phosphorylated H2AX (γH2AX), and cell cycle by flow cytometry and immunostaining of Ser10-phosphorylated histone H3.

Results: The $p53^{-/-}$ cells were more resistant than the $p53^{+/+}$ cells to X-ray irradiation, while the sensitivities of the $p53^{+/+}$ and $p53^{-/-}$ cells to carbon-ion beam irradiation were comparable. X-ray and carbon-ion beam irradiations predominantly induced apoptosis of the $p53^{+/+}$ cells but not the $p53^{-/-}$ cells. In the $p53^{-/-}$ cells, carbon-ion beam irradiation, but not X-ray irradiation, markedly induced mitotic catastrophe that was associated with premature mitotic entry with harboring long-retained DSBs at 24 h post-irradiation.

Conclusions: Efficient induction of mitotic catastrophe in apoptosis-resistant p53-deficient cells implies a strong cancer cell-killing effect of carbon-ion beam irradiation that is independent of the p53 status, suggesting its biological advantage over X-ray treatment.

Introduction

Carbon-ion radiotherapy has been provoking interest in the field of cancer therapy. Carbon-ion beams have advantageous properties over X-ray; a superior dose distribution associated with the sharp penumbra and the Bragg peak, and strong cell-killing effect [1, 2]. The major promising clinical outcome of carbon-ion radiotherapy is to overcome the therapeutic resistance of cancer cells to X-ray radiotherapy. For example, a recent study in which carbon-ion radiotherapy was used to treat patients with rectal cancer reported a 5-year local control and overall survival rates of 97% and 51% for post-operative recurrent cases [3]. This rate is superior to the 5-year overall survival rates (0−40%) that are typically achieved by conventional X-ray radiotherapy or surgical resection [3, 4]. However, the biological basis for the strong cell-killing effect of carbon-ion beam irradiation on X-ray-resistant tumors has not been elucidated fully.

Genetic aberrations contribute to the X-ray resistance of cancer cells [5, 6]. Inactivating mutations in the tumor suppressor gene *TP53* are representative of tumor resistance, and these aberrations are associated with poor prognosis after X-ray radiotherapy [7, 8]. The p53 protein plays multiple roles in the DNA damage response (DDR) to X-ray irradiation, including the regulation of cell death pathways and cell cycle checkpoints [9]. The induction of apoptosis by p53 is a key factor affecting the sensitivity of cancer cells to X-ray radiation. Several pre-clinical and clinical studies have demonstrated that *TP53* mutations are associated with the resistance of cancer cells to X-ray irradiation therapy [7, 10, 11].

Previous studies showed that carbon-ion beam irradiation effectively kills X-ray-resistant p53-mutant cancer cells [12—15]. Although the mechanisms involved in this process were examined in these studies, the results were inconsistent. The inconsistencies are likely attributable to the fact that each study focused on only a few aspects of the DDR (such as apoptosis or the cell cycle response) [12–15] and each used cancer cell lines with different genetic backgrounds; hence, the effects of aberrations in genes other than *TP53* may have masked the results [12, 13]. Here, to clarify the mechanisms underlying the strong killing effect of carbon-ion beam irradiation on X-ray irradiation-resistant cancer cells with *TP53* aberrations, we performed a comprehensive study of multiple aspects of the DDR using a set of isogenic human cancer cells that differed only in their p53 status.

Materials and Methods

Cell lines

Human colorectal cancer HCT116 cells harboring wild-type p53 ($p53^{+/+}$) and its isogenic p53-null derivative ($p53^{-/-}$) were provided by Dr. B. Vogelstein of Johns Hopkins University. HCT116 $p53^{+/+}$ cells have intact DNA damage checkpoints [16]. p53 expression, and the effects of X-ray and carbon-ion beam irradiation on p53 expression in $p53^{+/+}$ and $p53^{-/-}$ cells, was examined by immunoblotting with

antibodies against p53 (Santa Cruz) and β-actin (loading control, Cell Signaling Technology) (S1a Fig.). There was no significant difference in the population doubling time between the two cell lines (S1b Fig.).

Human colon cancer (RKO, LS123, and WiDr) cells, human lung cancer (H1299) cells, and human osteosarcoma (Saos-2) cells were purchased from ATCC. RKO cells harbor wild-type p53. LS123 and WiDr cells harbor a missense mutation in p53 at R175H and R273H, respectively. H1299 and Saos-2 cells are p53-null. H1299 cells stably expressing a p53 missense mutation (R175H, R273H, R249S or R280K) were established as described previously [17]. All cells were cultured in RPMI-1640 medium supplemented with 10% fetal bovine serum.

hTERT-immortalized normal human diploid foreskin fibroblasts (BJ-hTERT) harboring wild-type p53 were purchased from Clontech. BJ-hTERT cells expressing shRNA against EGFP (BJ-hTERT-WT; control) or p53 (BJ-hTERT-shp53) were established as previously described [18], and cultured in Minimum Essential Eagle's Medium.

Irradiation

X-ray irradiation was performed using a Faxitron RX-650 radiation source (100 kVp, 1.14 Gy/min; Faxitron Bioptics). Carbon-ion beam irradiation was performed at Gunma University Heavy Ion Medical Center using the same beam specifications that are used in clinical settings (290 MeV/nucleon and an average linear energy transfer (LET) at the center of a 6 cm spread-out Bragg peak of approximately 50 keV/μm). Carbon-ion beams were delivered in a vertical direction so that cells on culture plates can receive the dose evenly.

Clonogenic survival assay

Cells were seeded into 6-well plates and exposed (or not) to X-ray or carbon-ion beam irradiation. After incubation for a further 10 days, the cells were fixed with methanol and stained with crystal violet. Colonies of at least 50 cells were counted. The surviving fraction was normalized to the corresponding controls. The dose that resulted in a surviving fraction of 10% (D_{10}) was calculated using the linear-quadratic model, as described previously [19].

Cell death evaluations

Cells were grown on glass coverslips, exposed (or not) to X-ray or carbon-ion beam irradiation, and then stained with 4',6-diamidino-2-phenylindole dihydrochloride (DAPI), as described previously [20]. Confocal images were collected using a BX51 microscope (Olympus) equipped with a CCD camera (VB-7000; Keyence). Apoptosis was determined based on the morphology of the nuclei, including the presence of apoptotic bodies, nuclear condensation and fragmentation [21]. Cells containing nuclei with two or more distinct lobes were scored as positive for mitotic catastrophe [20, 22]. Cells containing nuclei showing

senescence-associated heterochromatic foci were scored as positive for senescence [23]. The percentages of cells undergoing apoptosis, mitotic catastrophe or senescence were quantified by counting at least 300 cells for each experimental condition.

Cell cycle analysis

Cells exposed (or not) to X-ray or carbon-ion beam irradiation were harvested at the indicated time points, fixed with ethanol, stained with propidium iodide in the presence of RNase, and then analyzed using flow cytometry, as described previously [19].

Immunostaining

Cells exposed (or not) to X-ray or carbon-ion beam irradiation were stained with antibodies against Ser139-phosphorylated histone H2AX (γH2AX; Millipore) or Ser10-phosphorylated histone H3 (pH3; Millipore), as described previously [24]. γH2AX foci per nucleus were scored in sequential 2D images captured from multiple focal planes. At least 500 cells were evaluated for each experimental condition.

Statistical analysis

Experiments were performed in triplicate at least unless otherwise stated. Statistically significant differences were determined by unpaired Student's *t*-tests using StatMateIII ver. 3.17 software (ATMS). $P<0.05$ was considered significant.

Results

Carbon-ion beams have more potent cancer cell-killing activity than X-rays irrespective of the p53 status

The sensitivities of $p53^{+/+}$ and $p53^{-/-}$ HCT116 cells to X-ray and carbon-ion beam irradiation were assessed by clonogenic survival assays (Fig. 1). As expected based on the results of previous studies [14, 15], $p53^{-/-}$ cells were more resistant to X-ray irradiation than $p53^{+/+}$ cells; the D_{10} values for these two cell lines were 6.8 Gy and 3.8 Gy, respectively. By contrast, the sensitivities of $p53^{+/+}$ and $p53^{-/-}$ cells to carbon-ion beam irradiation were comparable; the D_{10} values for these cell lines were 1.7 Gy and 1.9 Gy, respectively. Hence, the relative biological effectiveness of carbon-ion beam irradiation to X-ray irradiation at D_{10} was 2.2 in $p53^{+/+}$ cells and 3.6 in $p53^{-/-}$ cells. These data indicate that carbon-ion beam irradiation effectively kills X-ray-resistant *p53*-null cancer cells.

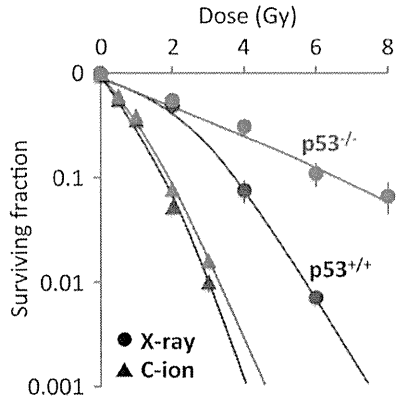

Fig. 1. Sensitivity of $p53^{+/+}$ and $p53^{-/-}$ HCT116 cells to X-ray and carbon-ion beam irradiation as assessed by clonogenic survival assays. Cells were seeded in 6-well plates, incubated overnight, and then exposed to X-ray or carbon-ion beam irradiation. After incubation for a further 10 days, the cells were fixed, stained, and counted. The surviving fraction was normalized to the value of the corresponding controls. Data are expressed as the mean ± SD. C-ion, carbon-ion.

doi:10.1371/journal.pone.0115121.g001

Aberrations in p53 switch the mode of irradiation-induced cancer cell death from apoptosis to mitotic catastrophe

To explore the mechanisms underlying the p53 status-independent cell-killing activity of carbon-ion beam irradiation, the modes of cell death induced by X-ray or carbon-ion beam irradiation were assessed (Figs. 2, 3). $p53^{+/+}$ and $p53^{-/-}$ cells were irradiated with doses of X-ray or carbon-ion beams that were similar to the D_{10} for $p53^{+/+}$ cells (X-ray, 4 Gy; carbon-ion beams, 1.5 Gy). Apoptosis, mitotic catastrophe and senescence were determined by examining the characteristic morphologies of nuclei stained with DAPI (Fig. 2a–c) [20–23]. In $p53^{+/+}$ cells, apoptosis was the dominant mode of cell death induced by X-ray and carbon-ion beam irradiation (Figs. 2d, f, 3a). By contrast, $p53^{-/-}$ cells were less susceptible to apoptosis caused by both types of irradiation (Figs. 2e, g, 3b). Interestingly, in $p53^{-/-}$ cells, carbon-ion beam irradiation induced mitotic catastrophe more evidently than X-ray irradiation (Figs. 2g, 3b). A higher dose of X-ray irradiation equivalent to the D_{10} (6.8 Gy) for $p53^{-/-}$ cells induced a similar level of mitotic catastrophe to that induced by carbon-ion beam irradiation at 1.5 Gy (S2 Fig.). The induction of senescence was not evident in all experimental conditions (Fig. 2). This result was confirmed by senescence-associated β-galactosidase staining assays, in which the fraction of staining-positive cells was less than 2% for both cell lines exposed to X-ray or carbon-ion beam irradiation (data not shown). These data indicated that apoptosis and mitotic catastrophe is the major mode of cell death in $p53^{+/+}$ cells and $p53^{-/-}$ cells, respectively, both after exposure to X-ray and carbon-ion beam irradiation, and that carbon-ion beam irradiation induces mitotic catastrophe more effectively than X-ray irradiation in apoptosis-resistant $p53^{-/-}$ cells.

To investigate this further, we examined the mode of cell death in multiple human cell lines with differing p53 status after X-ray or carbon-ion beam

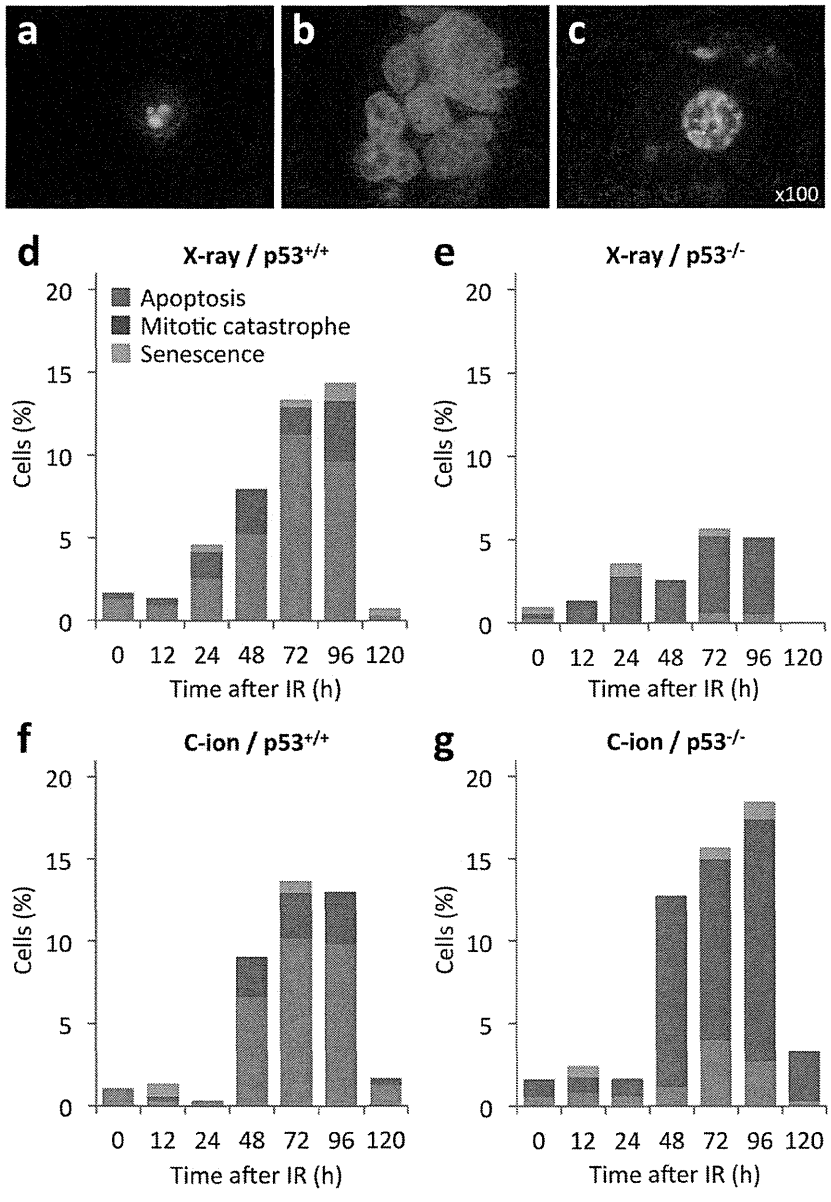

Fig. 2. Mode of cell death induced by X-ray or carbon-ion beam irradiation in $p53^{+/+}$ and $p53^{-/-}$ HCT116 cells. Cells seeded on glass coverslips were incubated overnight, exposed (or not; 0 h) to X-ray (4 Gy) or carbon-ion beam (1.5 Gy) irradiation, and then stained with DAPI. Apoptosis, mitotic catastrophe, and senescence were determined according to the characteristic nuclear morphologies (see "Materials and methods" for the definitions). (**a–c**) Representative images showing the nuclear morphology of cells undergoing apoptosis (a), mitotic catastrophe (b), or senescence (c). The images of $p53^{-/-}$ cells were taken 72 h after carbon-ion beam irradiation. (**d, e**) Mode of cell death in $p53^{+/+}$ (d) and $p53^{-/-}$ (e) cells at 0, 12, 24, 48, 72, 96 and 120 h after X-ray irradiation. (**f, g**) Mode of cell death in $p53^{+/+}$ (f) and $p53^{-/-}$ (g) cells at 0, 12, 24, 48, 72, 96 and 120 h after carbon-ion beam irradiation. IR, irradiation; C-ion, carbon-ion.

doi:10.1371/journal.pone.0115121.g002

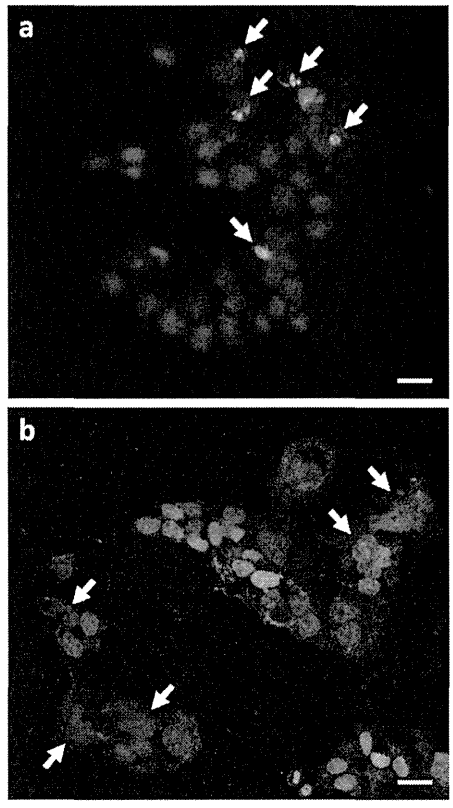

Fig. 3. Representative images of $p53^{+/+}$ and $p53^{-/-}$ HCT116 cells irradiated with carbon-ion beams. Cells were seeded on glass coverslips, incubated overnight, exposed to carbon-ion beams (1.5 Gy), and then stained with DAPI 72 h later. Apoptosis, mitotic catastrophe, and senescence were determined according to the characteristic nuclear morphologies (see "Materials and methods" for the definitions). (**a**) $p53^{+/+}$ cells: 12.5%, 0% and 0% of cells showed apoptosis, mitotic catastrophe, and senescence, respectively. (**b**) $p53^{-/-}$ cells: 0%, 12.8% and 0% of cells showed apoptosis, mitotic catastrophe, and senescence, respectively. The arrows in (a) and (b) indicate cells undergoing apoptosis and mitotic catastrophe, respectively. Scale bars, 10 μm.

doi:10.1371/journal.pone.0115121.g003

irradiation (Fig. 4). RKO cells harboring wild-type p53 showed an apoptosis-dominant phenotype after either X-ray or carbon-ion beam irradiation, whereas p53-null H1299 and Saos-2 cells showed a mitotic catastrophe-dominant phenotype. Accordingly, suppression of p53 expression in BJ-hTERT fibroblasts promoted the induction of mitotic catastrophe upon X-ray or carbon-ion beam irradiation (S3 Fig.). Interestingly, LS123 and WiDr cells (expressing p53 harboring a missense at R175H and R273H, respectively), also showed a mitotic catastrophe-dominant phenotype (Fig. 4). These mutation sites are located within the DNA-binding domain of the p53 protein, which plays a key role in the transcriptional activation of several target genes, including those involved in apoptosis induction [25]. Therefore, we next examined the mode of irradiation-induced cell death using a series of isogenic H1299 cells stably expressing p53 proteins harboring missense mutations in the DNA-binding domain that are often observed in human cancers (i.e., R175H, R273H, R249S and R280K) [25]. All of

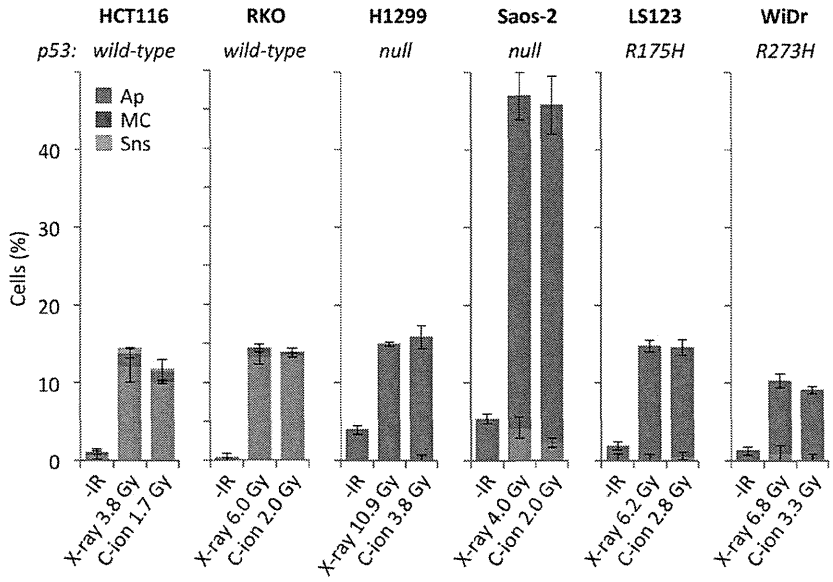

Fig. 4. Mode of cell death induced by X-ray or carbon-ion beam irradiation in cancer cell lines with differing *p53* status. Cells were seeded on glass coverslips, incubated overnight, irradiated with X-rays (D_{10} dose) or carbon-ion beams (D_{10} dose), and then stained with DAPI 72 h later. Apoptosis, mitotic catastrophe, and senescence were determined according to the characteristic nuclear morphologies (see "Materials and methods" for the definitions). Data are expressed as the mean ± SD. Ap, apoptosis; MC, mitotic catastrophe; Sns, senescence; IR, irradiation; C-ion, carbon-ion.

doi:10.1371/journal.pone.0115121.g004

these cell lines showed a mitotic catastrophe-dominant phenotype upon irradiation (Fig. 5). Taken together, these results indicate that dysfunction of the p53 DNA-binding domain switches the mode of irradiation-induced cancer cell death from apoptosis to mitotic catastrophe. These results also confirmed that carbon-ion beam irradiation was better than X-ray irradiation at inducing mitotic catastrophe in cancer cells harboring aberrant p53.

Cells are released from radiation-induced G2/M arrest 24 h after X-ray or carbon-ion beam irradiation

Mitotic catastrophe is thought to occur when cells proceed through aberrant mitosis with unrepaired DNA damage [26]. Therefore, to explore the mechanism underlying the induction of mitotic catastrophe in p53-null cells by carbon-ion beam irradiation, the effects of X-ray and carbon-ion beam irradiation on the cell cycle statuses of $p53^{+/+}$ and $p53^{-/-}$ HCT116 cells were determined by flow cytometry (Fig. 6a, b). Like the cell death analyses, the cells were irradiated with doses of X-ray (4 Gy) or carbon-ion beams (1.5 Gy). The induction of G2/M arrest that peaked 12 h after irradiation was observed in both cell lines after X-ray or carbon-ion beam irradiation, being more evident in the $p53^{-/-}$ cells than $p53^{+/+}$ cells. Notably, in both cell lines exposed to X-ray or carbon-ion beam irradiation, the G2/M arrest was fully released 48 h after irradiation.

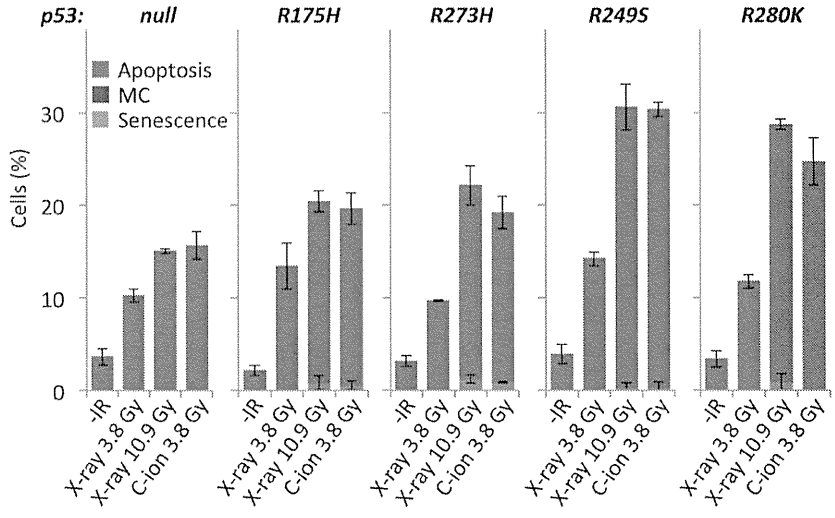

Fig. 5. Mode of cell death induced by X-ray or carbon-ion beam irradiation in isogenic H1299 cells expressing different p53 missense mutations. Cells were seeded on glass coverslips, incubated overnight, irradiated with X-rays (10.9 Gy, D_{10} for X-rays; or 3.8 Gy, D_{10} for carbon-ion beams) or carbon-ion beams (3.8 Gy, D_{10} for carbon-ion beams), and then stained with DAPI 72 h later. Apoptosis, mitotic catastrophe, and senescence were determined according to the characteristic nuclear morphologies (see "Materials and methods" for the definitions). Data are expressed as the mean ± SD. MC, mitotic catastrophe; C-ion, carbon-ion; IR, irradiation. Note that a part of p53-null H1299 panel is the same as that shown in Fig. 4 (but the context is now different).

doi:10.1371/journal.pone.0115121.g005

Next, the percentages of $p53^{+/+}$ and $p53^{-/-}$ cells in the M phase before and after X-ray (4 Gy) or carbon-ion beams (1.5 Gy) irradiation were assessed by immunostaining using an antibody against pH3 (Fig. 6c) [24]. Approximately 2% of non-irradiated $p53^{+/+}$ and $p53^{-/-}$ cells were in the M phase. One hour after carbon-ion beam irradiation, the percentages of these cells in the M phase were reduced significantly, although $p53^{-/-}$ cells were less susceptible than $p53^{+/+}$ cells to X-ray irradiation. Notably, 24 h after X-ray or carbon-ion beam irradiation, the percentages of $p53^{+/+}$ and $p53^{-/-}$ cells in the M phase recovered to the baseline, suggesting that both cell lines restarted mitosis 24 h after the treatment.

DNA double-strand breaks generated by carbon-ion beam irradiation show slower repair kinetics than those generated by X-ray irradiation

Finally, the repair kinetics of DNA double-strand breaks (DSBs), the most lethal type of DNA damage generated by ionizing irradiation, were examined in $p53^{+/+}$ and $p53^{-/-}$ HCT116 cells [27]. Irradiated cells were subjected to immunostaining using an antibody against γH2AX, and the numbers of γH2AX foci per cell at 15 min and 24 h post-irradiation were counted (Fig. 7, S1 Table) [24, 28]. The cells were irradiated with a 2 Gy dose of X-ray or a 1 Gy dose of carbon-ion beams; at these doses, the number of γH2AX foci per cell at the control time point (15 min post-irradiation) was approximately 20–30, which was appropriate for

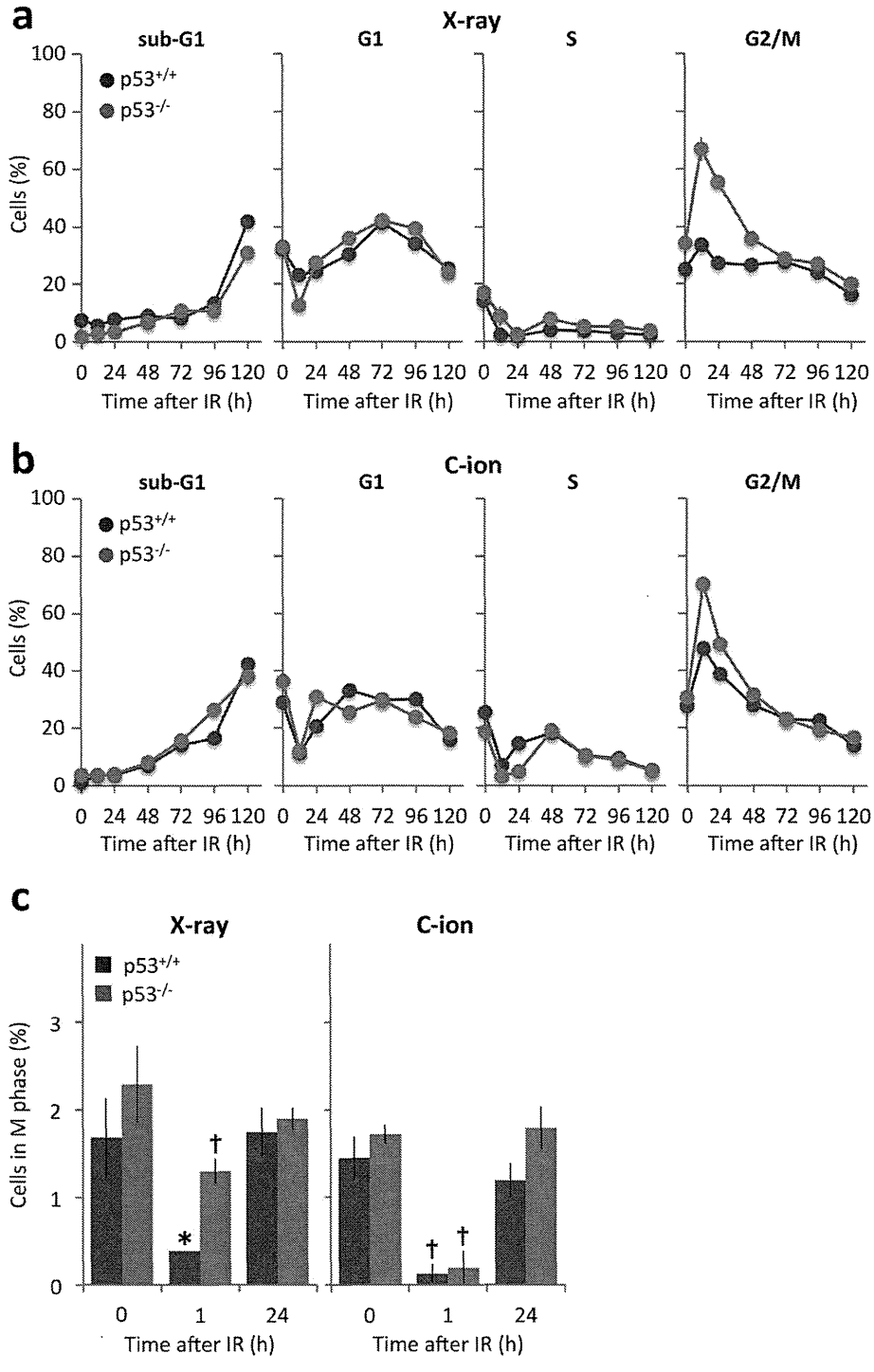

Fig. 6. Cell cycle profiles of $p53^{+/+}$ and $p53^{-/-}$ HCT116 cells irradiated with X-rays or carbon-ion beams. Cells were seeded in 35 mm culture plates (a, b) or on glass coverslips (c), incubated overnight, and exposed (or not; 0 h) to X-ray (4 Gy) or carbon-ion beam (1.5 Gy) irradiation. (**a, b**) Cells irradiated with X-rays (a) or carbon-ion beams (b) were incubated for 0, 12, 24, 48, 72, 96 or 120 h, fixed with ethanol, stained with propidium iodide, and cell cycle status analyzed by flow cytometry. (**c**) Cells were irradiated with X-rays or carbon-ion beams, incubated for 1 h, and then subjected to immunostaining for pH3, a specific marker for M

phase cells. Data are expressed as the mean ± SD. *$P<0.05$ and †$P<0.01$ versus the corresponding controls. IR, irradiation; C-ion, carbon-ion.

doi:10.1371/journal.pone.0115121.g006

the assessment [24, 28]. Twenty four hours after X-ray irradiation, the numbers of γH2AX foci in $p53^{+/+}$ and $p53^{-/-}$ cells were 24 ± 4.3% and 23 ± 5.3% of those of the corresponding controls (at the 15 min time point), respectively (Fig. 7a, b), indicating that the large number of DSBs generated by X-ray irradiation were repaired within 24 h. By contrast, 24 h after carbon-ion beam irradiation, the numbers of γH2AX foci in $p53^{+/+}$ and $p53^{-/-}$ cells were 93 ± 11% and 85 ± 7.3% of those of the corresponding controls, respectively (Fig. 7a, c), indicating that the DSBs generated by carbon-ion beam irradiation were not repaired efficiently, probably due to the structural complexity of DSB ends [29]. Indeed, $p53^{+/+}$ and $p53^{-/-}$ cells that stained double-positive for γH2AX and pH 3 were identified 24 h after carbon-ion beam irradiation, demonstrating that cells harboring DSBs had entered mitosis (Fig. 7d). The p53 status did not affect the kinetics of the loss of γH2AX foci after X-ray or carbon-ion beam irradiation. Taken together, these data suggest that p53-null cells harboring unrepaired DSBs enter mitosis 24 h after carbon-ion beam irradiation, leading to mitotic catastrophe.

Discussion

Here, we demonstrate that carbon-ion beam irradiation induces distinct modes of cell death according to the mutation status of *TP53*. After both X-ray and carbon-ion beam irradiation, apoptosis was the dominant mode of cell death of $p53^{+/+}$ cells but not $p53^{-/-}$ cells. Notably, the rate of mitotic entry and the kinetics of DSB repair after irradiation, which may be key factors that induce mitotic catastrophe, were similar in $p53^{+/+}$ and $p53^{-/-}$ cells regardless of the type of irradiation used. These data indicate that apoptosis plays a primary role in cancer cell death caused by irradiation in the presence of p53. In the absence of p53, cancer cells showed resistance to apoptosis induction and mitotic catastrophe was observed after both X-ray and carbon-ion beam irradiation. This finding is likely explained by limitation of the G2/M checkpoint after irradiation. Activation of this checkpoint allows the repair of damaged DNA before it is passed on to daughter cells and acts as a barrier to prevent premature entry into mitosis [30]. However, previous studies have suggested the limitation of G2/M checkpoint after IR; G2/M checkpoint is released when the number of DSBs becomes lower than ~10–20, followed by mitotic entry [24, 31]. Following the G2/M checkpoint release, cells harboring 10–20 DSBs are able to complete the mitotic event and enter the G1 phase [32, 33]. DSB repair is downregulated in the M phase; therefore, this damage may be repaired in the next cell cycle, although the repair process in daughter cells remains to be elucidated [34]. Another possible reason for the efficient induction of mitotic catastrophe in $p53^{-/-}$ cells is the higher propensity of these cells to stall in the G2/M phase after irradiation than $p53^{+/+}$ cells. This G2/M